JOURNAL OF AGRICULTURAL AND FOOD CHEMISTRY

Functional Structure/Activity Relationships

Synthesis and Activity of 1,2,3-Triazole Aminopyrimidines against Cyanobacteria as PDHc-E1 Competitive Inhibitors

Yuan Zhou, Jiangtao Feng, Lingling Feng, Dan Xie, Hao Peng, Meng Cai, and Hongwu He

J. Agric. Food Chem., **Just Accepted Manuscript** • DOI: 10.1021/acs.jafc.9b02878 • Publication Date (Web): 22 Oct 2019

Just Accepted

is published by the American Chemical Society. 1155 Sixteenth Street N.W., Washington, DC 20036

Synthesis and Activity of 1,2,3-Triazole Aminopyrimidines against Cyanobacteria as PDHc-E1 Competitive Inhibitors

Yuan Zhou[1], Jiangtao Feng[1], Lingling Feng, Dan Xie, Hao Peng, Meng Cai*, Hongwu He*

Key Laboratory of Pesticide and Chemical Biology of Ministry of Education, College of Chemistry, Central China Normal University, 152 Luoyu Road, Wuhan 430079, P. R. China

***CORRESPONDING AUTHOR FOOTNOTE**

To whom correspondence should be addressed. Tel./fax: +86 (0)27 67867960, E-mail addresses: he1208@mail.ccnu.edu.cn,cm122587@163.com.

[1] These authors equally contributed to this work.

Abstract

Cyanobacteria harmful algal blooms are of a global concern, but all currently available algicides in market are non-selective and have potential side effects on non-target species. In the present work, two series of compounds (**4** and **6**) comprising 16 novel 1,2,3-triazole aminopyrimidines were rational designed and synthesized as control agent for cyanobacteria. Our design focus was the inhibiting cyanobacteria by inhibition against pyruvate dehydrogenase complex E1 (PDHc-E1). Compounds **4** and **6** showed potent inhibition against *Escherichia coli* PDHc-E1 (IC_{50} = 4.13-23.76 μM) and also strong algicidal activities against *Synechocystis* sp. PCC 6803 (EC_{50} = 1.7-8.1 μM) and *Microcystis* sp. FACHB905 (EC_{50} = 2.1-11.8 μM). In particular, the algicidal activities of **6d** against four algal species were not only higher than that of prometryn; they were also comparable to or higher than that of copper sulfate. The analogs **4c**, **4d**, **6d**, and **6e** displayed potent algicidal activities and inhibition of *E. coli* PDHc-E1 but exhibited negligible inhibition of porcine PDHc-E1. As revealed by molecular docking, site-directed mutagenesis, enzymatic assays, and an inhibition kinetic analysis, **4c** and **6d** inhibited PDHc-E1 in a competitive manner. Our results suggest that highly selective, effective algicides can be developed by rationally designing competitive PDHc-E1 inhibitors.

Keywords: synthesis; PDHc-E1 inhibitor; anti-cyanobacteria; selectivity; molecular docking

1 Introduction

Along with increasing eutrophication and global warming, cyanobacteria harmful algal blooms (Cyano-HABs) have become a worldwide concern.[1-3] Cyano-HABs can destroy aquatic ecosystems by depleting oxygen levels, with cyanobacteria themselves producing cyanotoxins that threaten aquatic organism survival and human health.[4, 5] An urgent need to control Cyano-HABs therefore exists. One of the most convenient control methods is the application of chemicals.[6, 7] Applied chemicals include inorganic copper fungicides (e.g., copper sulfate, copper oxychloride, and copper citrate), herbicides (e.g., prometryne, diquat, paraquat, atrazine, and simazine), and chemical oxidants (e.g., chlorine dioxide, hydrogen peroxide, potassium permanganate, and calcium peroxide).[8] Unfortunately, all currently available algicides in market are non-selective and have potential side effects on non-target species, including human beings. This non-selectivity has served as the impetus for designing chemicals that target unique enzymes of cyanobacteria.

Pyruvate dehydrogenase E1 (PDHc-E1), a member of the pyruvate dehydrogenase complex, catalyzes the only irreversible step of a multistep process using thiamine diphosphate (ThDP) and Mg^{2+} as cofactors.[9] PDHc-E1 is therefore a feasible target for the evaluation of novel algicides. Given the indispensability of ThDP in pyruvate metabolism in microbe,[10, 11] the design and synthesis of ThDP analogs as PDHc-E1 inhibitors may be a good strategy for the discovery of novel algicides.

We thus aimed to design an algicide that can selectively inhibit PDHc-E1. Cyanobacteria and *Escherichia coli*, which are both prokaryotes, have nuclei without nuclear membranes and lack membrane-bound plastids. Because the crystal structure of cyanobacterial PDHc-E1 has not been reported, we were only able to design new inhibitors against PDHc-E1 from *E. coli* (PDB code:

1L8A).[12] We first synthesized a series of 1,2,3-triazole aminopyrimidines **I** (**Fig. 1**) and demonstrated their effectiveness as inhibitors against *E. coli* PDHc-E1.[13] However, these compounds displayed poor algicidal activity. Compounds **II**, **III** and **IV** (**Fig. 1**) were then synthesized by modifying the phenoxy moiety of **I**. Most of these new compounds showed potent inhibition against both *E. coli* PDHc-E1 and cyanobacteria that was significantly superior to **I**.[14] Particularly, compound **IV-21l** (R^1= I, R = 6-Br) (**Fig.1**) has the best inhibition against the cyanobacteria strain *Synechocystis* sp. PCC6803 with an EC_{50} of 0.7 μM.[14] However, the synthesis process of this compound is complicated, and its water- and fat-solubility is poor because of its three different nitro-containing heterocycles. These findings encouraged us to design more potent PDHc-E1 inhibitors by modifying **I** with the aid of *E. coli* PDHc-E1 structure-based molecular docking methods. The molecular docking analysis indicated that the "linker portion" between the 1,2,3-triazole and benzene ring of **I** could not form hydrogen bonds with any amino acid residues in the active site of *E. coli* PDHc-E1. We hypothesized that the formation of a hydrogen bond between the "linker portion" and the amino acid residues in the active site should be greatly beneficial for enhancing inhibition against *E. coli* PDHc-E1. For this purpose, we considered an imine or amide group containing a NH or C=O moiety, which could be used as a hydrogen donor (NH) or receptor (C=O). Our recent work has therefore focused on using an imine or amide group as the "linker portion" to obtain a novel series of 5-((4-((substituted amino)methyl)-1*H*-1,2,3-triazol-1-yl)methyl)- 2-methylpyrimidin-4-amine (**4**) and 1-((4-amino-2-methylpyrimidin-5-yl)methyl)-*N*-substituted-1*H*-1,2,3-triazole-4-carboxamide (**6**) compounds (**Fig. 2**).

Here, we report the chemical synthesis of the 2 series of compounds (**4** and **6**) and their

biological activities against *E. coli* PDHc-E1 and five algal species (*Synechocystis* sp. PCC6803, *Microcystis* sp. FACHB905, *Anabaena* sp. FACHB82, *Aphanizomenon* sp. FACHB1395, and *Nostoc* sp. FACHB713).

2 Material and Methods

2.1 Chemistry

All melting points (m.p.) were determined with a digital model X-5 apparatus (uncorrected). ^{1}H and ^{19}F nuclear magnetic resonance (NMR) spectra were recorded on a Bruker spectrometer at 400 MHz and 376 MHz with tetramethylsilane as the internal standard. Chemical shifts were reported in δ (ppm) (parts per million) values. A MicroMass GCT CA 055 instrument was used to acquire high-resolution electron impact mass spectra (HR-EIMS) under electron impact (70 eV) conditions. Elemental analyses were performed on a Vario ELIIICHNSO element analyzer, and crystal structures were obtained with Bruker AEPEX DUO CCD diffractometer. All chemicals and reagents used for syntheses were purchased from commercial sources; they were of AR grade and used without further purification.

2.2 Procedure for the preparation of 5-azidomethyl-2-methylpyrimidine-4-yl-amine 1.

As described by Erixon,[15] a stirring suspension of 30.6 mmol thiamine chloride (Vitamin B1), 75.4 mmol sodium azide and 3.0 mmol sodium sulfite in water (100mL) was heated at 65 ^{o}C. After 5 h, 100 mmol citric acid (pH ≈ 4) was added into the aqueous solution. The reaction mixture was stirred at room temperature. After 30 min, potassium carbonate was added until the pH value reached 8.0. A white precipitation of the product began forming immediately. The suspension was thoroughly stirred and filtered. The filter cake was washed with saturated potassium carbonate solution and dried to afford a white solid (Yield: 65%, m.p. 150-152 ^{o}C).

2.3 General procedure for preparation of *N*-(prop-2-yn-1-yl)anilines 3.

According to the procedure described by Majumdar,[16] to a stirred suspension of an appropriate substituted aniline **2** (12 mmol) and potassium carbonate (10 mmol) in dry DMF (15 mL) was added propargyl bromide (10 mmol). The reaction mixture was stirred at room temperature and monitored by thin layer chromatography (TLC). After the reaction finished, the reaction mixture was washed with water (15 mL) and extracted with EtOAc (60 mL). The combined organic extracts were then washed with brine (20 mL), dried over Na_2SO_4, and concentrated *in vacuo*. The crude products was further purified by a silica gel column using a 1:20 (v/v) acetate/petroleum ether mixture as the eluent, which afforded the corresponding *N*-(prop-2-yn-1-yl)aniline **3**. A series of **3** could be obtained by this procedure in the yields of 72-85 %.

2.4 General procedure for preparation of *N*-phenylpropiolamides 5.

Compounds **5** were synthesized *via* the method repoted by Ramachandran.[17] To a stirred suspension of dicyclohexylcarbodiimide (DCC) (12 mmol) in dichloromethane (DCM) (50 mL), propiolic acid was added slowly at -5 ^{o}C ~ 0 ^{o}C. After 1 h of stirring at 0 ^{o}C, a solution of substituted aniline (10 mmol) in DCM (20 mL) was added to the reaction mixture and then stirred at room temperature for 24 h. After the reaction finished, the reaction mixture was filtered and the filtrate was evaporated *in vacuo*. The residue was purified by a silica gel column using a 1:50 (v/v) ethyl acetate/petroleum ether as the eluent, which afforded the corresponding *N*-phenylpropiolamide **5**. A series of **5** could be obtained by this procedure in the yields of 53-79%.

2.5 General procedure for the synthesis of 1,2,3-triazole aminopyrimidines 4 and 6.

To a stirring suspension of **1** (2 mmol) and an appropriate intermediate **3** or **5** (2 mmol) in THF, CuI (0.2 mmol) and Et_3N (2.4 mmol) were added sequentially. The reaction mixture was stirred at room temperature for overnight prior the addition of water (30 mL). The product suspension was filtered and dried. The filter cake was further purified by recrystallization (methanol/dichloromethane) to give corresponding title compound **4** or **6**. Two series of **4** and **6** could be obtained by same procedure.

2.5.1 2-methyl-5-((4-((phenylamino)methyl)-1*H*-1,2,3-triazol-1-yl)methyl)pyrimidin-4-amine (4a)

Yellow solid; Yield 57%; m.p.188-189 °C; ^{1}H NMR (400 MHz, DMSO-d_6) δ(ppm): 2.29 (s, 3H, CH_3), 4.24 (d, J = 5.4 Hz, 2H, CH_2), 5.37 (s, 2H, CH_2), 6.03 (s, 1H, Ar-H), 6.51 (t, J = 7.0 Hz, 1H, Ar-H), 6.58 (d, J = 7.8 Hz, 2H, Ar-H), 6.91 (s, 2H, Ar-H, 1,2,3-trizole), 7.03 (t, J = 7.4 Hz, 2H, NH, pyrimidine-H), 7.93 (s, 2H, NH_2); HRMS (ESI): calcd. for $C_{15}H_{17}N_7$ $[M+H]^+$ 296.16182, found: 296.16210; Elemental Anal. Calcd for $C_{15}H_{17}N_7$: C, 61.00; H, 5.80; N, 33.20. Found: C, 60.87; H, 5.91; N, 32.75.

2.5.2 5-((4-(((2-chlorophenyl)amino)methyl)-1*H*-1,2,3-triazol-1-yl)methyl)-2-methylpyrimidin-4-amine (4b)

Yellow solid; Yield 60%; m.p.136-138 °C; ^{1}H NMR (400 MHz, DMSO-d_6) δ(ppm): 2.29 (s, 3H, CH_3), 4.39 (d, J = 5.5 Hz, 2H, CH_2), 5.36 (s, 2H, CH_2), 5.90 (t, J = 5.6 Hz, 1H, Ar-H), 6.55 (t, J = 7.1 Hz, 1H, Ar-H), 6.71 (d, J = 8.3 Hz, 1H, Ar-H), 6.91 (s, 2H, Ar-H, 1,2,3-triazole-H), 7.05 (t, J = 7.4 Hz, 1H, NH), 7.21 (d, J = 7.6 Hz, 1H, pyrimidine-H), 7.92 (s, 2H, NH_2); HRMS (ESI): calcd. for $C_{15}H_{16}ClN_7$ $[M+H]^+$ 330.12285, found: 330.12283; Elemental Anal. Calcd for

$C_{15}H_{16}ClN_7$: C, 54.63; H, 4.89; N, 29.73. Found: C, 54.71; H, 4.95; N, 29.64.

2.5.3

5-((4-(((3-chlorophenyl)amino)methyl)-1*H*-1,2,3-triazol-1-yl)methyl)-2-methylpyrimidin-4-amine (4c)

Yellow solid; Yield 67%; m.p.149-151 °C; ^{1}H NMR (400 MHz, DMSO-d_6) δ(ppm): 2.32 (s, 3H, CH_3), 4.30 (d, J = 5.7 Hz, 2H, CH_2), 5.44 (s, 2H, CH_2), 6.46 (t, J = 5.6 Hz, 1H, Ar-H), 6.51-6.63 (m, 2H, Ar-H), 6.66 (s, 1H, Ar-H), 6.97 (s, 2H, 1,2,3-triazole-H, pyrimidine-H), 7.08 (t, J = 8.0 Hz, 1H, NH), 8.01 (s, 2H, NH_2); HRMS (ESI): calcd. for $C_{15}H_{16}ClN_7$ $[M+H]^+$ 330.12285, found: 330.12276; Elemental Anal. Calcd for $C_{15}H_{16}ClN_7$: C, 54.63; H, 4.89; N, 29.73. Found: C, 54.55; H, 4.91; N, 29.81.

2.5.4

5-((4-(((4-chlorophenyl)amino)methyl)-1*H*-1,2,3-triazol-1-yl)methyl)-2-methylpyrimidin-4-amine (4d)

Yellow solid; Yield 72%; m.p.174-176 °C; ^{1}H NMR (400 MHz, DMSO-d_6) δ(ppm): 2.32 (s, 3H, CH_3), 4.26 (d, J = 3.9 Hz, 2H, CH_2), 5.45 (s, 2H, CH_2), 6.29 (s, 1H, Ar-H), 6.62 (d, J = 8.6 Hz, 2H, Ar-H), 6.97 (s, 2H, Ar-H, 1,2,3-triazole-H), 7.08 (d, J = 8.6 Hz, 2H, pyrimidine-H, NH), 7.98 (s, 2H, NH_2); HRMS (ESI): calcd. for $C_{15}H_{16}ClN_7$ $[M+H]^+$ 330.12285, found: 330.12296; Elemental Anal. Calcd for $C_{15}H_{16}ClN_7$: C, 54.63; H, 4.89; N, 29.73. Found: C, 54.56; H, 4.77; N, 29.75.

2.5.5

5-((4-(((3-bromophenyl)amino)methyl)-1*H*-1,2,3-triazol-1-yl)methyl)-2-methylpyrimidin-4-amine (4e)

Yellow solid; Yield 65%; m.p.143-145 °C; ^{1}H NMR (400 MHz, DMSO-d_6) δ(ppm): 2.29 (s, 3H, CH_3), 4.25 (d, J = 4.4 Hz, 2H, CH_2), 5.39 (s, 2H, CH_2), 6.31-6.46 (m, 1H, Ar-H), 6.61 (dd, J = 25.3, 7.1 Hz, 2H, Ar-H), 6.76 (s, 1H, Ar-H), 6.95 (dd, J = 19.2, 11.0 Hz, 3H, NH, 1,2,3-trizole-H, pyrimidine-H), 7.95 (s, 2H, NH_2); HRMS (ESI): calcd. for $C_{15}H_{16}BrN_7$ $[M+H]^+$ 374.07233, found: 374.07211; Elemental Anal. Calcd for $C_{15}H_{16}BrN_7$: C, 48.14; H, 4.31; N, 26.20. Found: C, 48.01; H, 4.42; N, 26.43.

2.5.6

2-methyl-5-((4-(((3-(trifluoromethyl)phenyl)amino)methyl)-1*H*-1,2,3-triazol-1-yl)methyl)pyrimidin-4-amine (4f)

Yellow solid; Yield 62%; m.p.144-146 °C; ^{1}H NMR (400 MHz, DMSO-d_6) δ(ppm): 2.32 (s, 3H, CH_3), 4.36 (s, 2H, CH_2), 5.43 (s, 2H, CH_2), 6.63 (s, 1H, Ar-H), 6.77-7.13 (m, 5H, Ar-H, 1,2,3-triazole-H, pyrimidine-H), 7.29 (s, 1H, NH), 8.02 (s, 2H, NH_2); ^{19}F NMR (376 MHz, DMSO-d_6) δ(ppm): -61.25; HRMS (ESI): calcd. for $C_{16}H_{16}F_3N_7$ $[M+H]^+$ 364.1492, found: 364.14954; Elemental Anal. Calcd for $C_{16}H_{16}F_3N_7$: C, 52.89; H, 4.44; N, 26.98. Found: C, 53.05; H, 4.51; N, 27.04.

2.5.7

2-methyl-5-((4-(((4-(trifluoromethyl)phenyl)amino)methyl)-1*H*-1,2,3-triazol-1-yl)methyl)pyrimidin-4-amine (4g)

Yellow solid; Yield 69%; m.p.150-152 °C; ^{1}H NMR (400 MHz, DMSO-d_6) δ(ppm): 2.28 (s, 3H, CH_3), 4.31 (s, 2H, CH_2), 5.39 (s, 2H, CH_2), 6.58 (s, 1H, Ar-H), 6.84 (d, J = 28.3 Hz, 5H, Ar-H, 1,2,3-triazole-H, pyrimidine-H), 7.24 (s, 1H, NH), 7.97 (s, 2H, NH_2); ^{19}F NMR (376 MHz, DMSO-d_6) δ(ppm): -61.24; HRMS (ESI): calcd. for $C_{16}H_{16}F_3N_7$ $[M+H]^+$ 364.1492, found:

364.14949; Elemental Anal. Calcd for $C_{16}H_{16}F_3N_7$: C, 52.89; H, 4.44; N, 26.98. Found: C, 52.71; H, 4.52; N, 26.84.

2.5.8 2-methyl-5-((4-((p-tolylamino)methyl)-1*H*-1,2,3-triazol-1-yl)methyl)pyrimidin-4-amine (4h)

Yellow solid; Yield 72%; m.p.75-77 ^{o}C; ^{1}H NMR (400 MHz, DMSO-d_6) δ(ppm): 2.32 (s, 6H, $2CH_3$), 4.44 (s, 2H, CH_2), 5.52 (s, 2H, CH_2), 7.01 (s, 1H, Ar-H), 7.21 (d, J = 28.3 Hz, 5H, Ar-H, 1,2,3-triazole-H, pyrimidine-H), 7.67 (s, 1H, NH), 8.68 (s, 2H, NH_2); HRMS (ESI): calcd. for $C_{16}H_{19}N_7$ $[M+H]^+$ 310.17747, found: 310.17727; Elemental Anal. Calcd for $C_{16}H_{19}N_7$: C, 62.12; H, 6.19; N, 31.69. Found: C, 59.98; H, 6.05; N, 31.64.

2.5.9

1-((4-amino-2-methylpyrimidin-5-yl)methyl)-*N*-phenyl-1*H*-1,2,3-triazole-4-carboxamide (6a)

Yellow solid; Yield 65%; m.p.249-251 ^{o}C; ^{1}H NMR (400 MHz, DMSO-d_6) δ(ppm): 2.33 (s, 3H, CH_3), 5.54 (s, 2H, CH_2), 7.06 (d, J = 32.0 Hz, 3H, Ar-H), 7.33 (s, 2H, Ar-H), 7.82 (s, 2H, NH_2), 8.10 (s, 1H, 1,2,3-triazole-H), 8.71 (s, 1H, pyrimidine-H), 10.45 (s, 1H, NH); HRMS (ESI): calcd. for $C_{15}H_{15}N_7O$ $[M+H]^+$ 310.14108, found: 310.14102; Elemental Anal. Calcd for $C_{15}H_{15}N_7O$: C, 58.24; H, 4.89; N, 31.70. Found: C, 58.38; H, 4.77; N, 31.58.

2.5.10

1-((4-amino-2-methylpyrimidin-5-yl)methyl)-*N*-(3-chlorophenyl)-1*H*-1,2,3-triazole-4-carboxamide (6b)

Yellow solid; Yield 78%; m.p.>260 ^{o}C; ^{1}H NMR (400 MHz, DMSO-d_6) δ(ppm): 2.31 (s, 3H, CH_3), 5.53 (s, 2H, CH_2), 6.98 (s, 2H, Ar-H), 7.13 (d, J = 7.4 Hz, 1H, Ar-H), 7.33 (d, J = 7.5 Hz, 1H, Ar-H), 7.73 (d, J = 8.2 Hz, 1H, 1,2,3-triazole-H), 7.97 (s, 2H, NH_2), 8.71 (s, 1H,

pyrimidine-H), 10.63 (s, 1H, NH); HRMS (ESI): calcd. for $C_{15}H_{14}ClN_7O$ $[M+H]^+$ 344.10211, found: 344.10201; Elemental Anal. Calcd for $C_{15}H_{14}ClN_7O$: C, 52.41; H, 4.10; N, 28.52. Found: C, 52.53; H, 4.05; N, 28.64.

2.5.11

1-((4-amino-2-methylpyrimidin-5-yl)methyl)-*N*-(4-chlorophenyl)-1*H*-1,2,3-triazole-4-carboxamide (6c)

Yellow solid; Yield 82%; m.p.>260 °C; ^{1}H NMR (400 MHz, DMSO-d_6) δ(ppm): 2.31 (s, 3H, CH_3), 5.54 (s, 2H, CH_2), 6.99 (s, 2H, Ar-H), 7.36 (d, J = 5.9 Hz, 2H, Ar-H), 7.82 (d, J = 6.2 Hz, 3H, NH_2, 1,2,3-triazole-H), 8.69 (s, 1H, pyrimidine-H), 10.59 (s, 1H, NH); HRMS (ESI): calcd. for $C_{15}H_{14}ClN_7O$ $[M+H]^+$ 344.10211, found: 344.10215; Elemental Anal. Calcd for $C_{15}H_{14}ClN_7O$: C, 52.41; H, 4.10; N, 28.52. Found: C, 52.26; H, 3.98; N, 28.44.

2.5.12

1-((4-amino-2-methylpyrimidin-5-yl)methyl)-*N*-(3-bromophenyl)-1*H*-1,2,3-triazole-4-carboxamide (6d)

White solid; Yield 77%; m.p.>260 °C; ^{1}H NMR (400 MHz, DMSO-d_6) δ(ppm): 2.34 (s, 3H, CH_3), 5.57 (s, 2H, CH_2), 7.04 (s, 2H, Ar-H), 7.32 (s, 2H, Ar-H), 7.83 (s, 1H, NH_2), 8.17 (s, 1H, 1,2,3-triazole-H), 8.76 (s, 1H, pyrimidine-H), 10.68 (s, 1H, NH); HRMS (ESI): calcd. for $C_{15}H_{14}BrN_7O$ $[M+H]^+$ 388.0516, found: 388.05113; Elemental Anal. Calcd for $C_{15}H_{14}BrN_7O$: C, 46.41; H, 3.63; N, 25.26. Found: C, 46.53; H, 3.55; N, 25.40.

2.5.13

1-((4-amino-2-methylpyrimidin-5-yl)methyl)-*N*-(4-bromophenyl)-1*H*-1,2,3-triazole-4-carboxamide (6e)

White solid; Yield 84%; m.p.>260 °C; ^{1}H NMR (400 MHz, DMSO-d_6) δ(ppm): 2.34 (s, 3H, CH_3), 5.56 (s, 2H, CH_2), 7.03 (s, 2H, Ar-H), 7.54 (d, J = 6.8 Hz, 2H, Ar-H), 7.83 (d, J = 7.1 Hz, 2H, NH_2), 8.12 (s, 1H, 1,2,3-triazole-H), 8.75 (s, 1H, pyrimidine-H), 10.65 (s, 1H, NH); HRMS (ESI): calcd. for $C_{15}H_{14}BrN_7O$ $[M+H]^+$ 388.0516, found: 388.05100; Elemental Anal. Calcd for $C_{15}H_{14}BrN_7O$: C, 46.41; H, 3.63; N, 25.26. Found: C, 46.27; H, 3.72; N, 25.14.

2.5.14

1-((4-amino-2-methylpyrimidin-5-yl)methyl)-*N*-(4-fluorophenyl)-1*H*-1,2,3-triazole-4-carboxamide (6f)

Yellow solid; Yield 71%; m.p.>260 °C; ^{1}H NMR (400 MHz, DMSO-d_6) δ(ppm): 2.32 (s, 3H, CH_3), 5.56 (s, 2H, CH_2), 7.02 (s, 2H, Ar-H), 7.18 (t, J = 7.7 Hz, 3H, Ar-H, , 1,2,3-triazole-H), 7.83 (s, 2H, NH_2), 8.71 (s, 1H, pyrimidine-H), 10.56 (s, 1H, NH); ^{19}F NMR (376 MHz, DMSO-d_6) δ(ppm): -118.62; HRMS (ESI): calcd. for $C_{15}H_{14}FN_7O$ $[M+H]^+$ 328.13166, found: 328.13175; Elemental Anal. Calcd for $C_{15}H_{14}FN_7O$: C, 55.04; H, 4.31; N, 29.95. Found: C, 54.87; H, 4.51; N, 30.08.

2.5.15

1-((4-amino-2-methylpyrimidin-5-yl)methyl)-*N*-(3-(trifluoromethyl)phenyl)-1*H*-1,2,3-triazole-4-carboxamide (6g)

White solid; Yield 76%; m.p.193-195 °C; ^{1}H NMR (400 MHz, DMSO-d_6) δ(ppm): 2.31 (s, 3H, CH_3), 5.53 (s, 2H, CH_2), 6.99 (s, 2H, Ar-H), 7.43 (d, J = 7.0 Hz, 1H, Ar-H), 7.50-7.67 (m, 1H, Ar-H), 8.06 (d, J = 7.6 Hz, 2H, NH_2), 8.28 (s, 1H, 1,2,3-triazole-H), 8.73 (s, 1H, pyrimidine-H), 10.80 (s, 1H, NH); ^{19}F NMR (376 MHz, DMSO-d_6) δ(ppm): -61.19; HRMS (ESI): calcd. for $C_{16}H_{14}F_3N_7O$ $[M+H]^+$ 378.12847, found: 378.12864; Elemental Anal. Calcd for $C_{16}H_{14}F_3N_7O$: C,

50.93; H, 3.74; N, 25.98. Found: C, 51.07; H, 3.55; N, 26.13.

2.5.16

1-((4-amino-2-methylpyrimidin-5-yl)methyl)-*N*-(*p*-tolyl)-1*H*-1,2,3-triazole-4-carboxamide (6h)

White solid; Yield 77%; m.p.245-247 ^{o}C; ^{1}H NMR (400 MHz, DMSO-d_6) δ(ppm): 2.31 (s, 3H, CH_3), 3.63 (s, 3H, CH_3), 5.61 (s, 2H, CH_2), 7.12 (d, J = 34.8 Hz, 4H, Ar-H), 7.72 (s, 3H, NH_2, 1,2,3-triazole-H), 8.73 (s, 1H, pyrimidine-H), 10.40 (s, 1H, NH); HRMS (ESI): calcd. for $C_{16}H_{17}N_7O$ $[M+H]^+$ 324.15673, found: 324.15644; Elemental Anal. Calcd for $C_{16}H_{17}N_7O$: C, 59.43; H, 5.30; N, 30.32. Found: C, 59.57; H, 5.55; N, 29.90.

2.6 Crystallographic study

A colorless single crystal of **4b** suitable for X-ray analysis was cultured from a mixture of methanol and dichloromethane at room temperature. Unit cell determination and data collection were performed using Mo Kα radiation (λ = 0.71073 Å) on a Bruker AEPEX DUO CCD diffractometer in π-ω scan mode at 298(2) K. The structure was solved directly using the SHELXS program of the SHELXTL package and refined by full-matrix least-squares methods with SHELXL. The position of all hydrogen atoms were determined from difference Fourier maps. All non-hydrogen atoms of **4b** were refined with anisotropic thermal parameters.

2.7 Enzyme inhibition assay for PDHc-E1

The preparation of PDHc-E1 from *E. coli* and the measurement of enzymatic activities were essentially as previously reported.[18] The half maximal inhibitory concentration (IC_{50}) was determined in a reaction mixture containing 50 mM K_3PO_4 (pH 6.4), 0.4 mM 2,6-dichlorophenolindophenol (DCPIP), 50 μM sodium pyruvate as the substrate, 5 μg PDHc-E1

purified enzyme, and 50 μM ThDP. Title compounds with different concentration gradients were incubated for 5 min with PDHc-E1 at 37 °C prior to addition of the pyruvate substrate. IC_{50} values were obtained from a nonlinear least-squares fitting of the data using the Hill kinetic equations under the Growth/Sigmoidal model in Origin 7.0 software as described previously.[19]

Site-directed mutations were introduced to PDHc-E1 using the Fast Mutagenesis System (TransGen Biotech, Beijing, China).The pMAL-c2X-PDHc-E1 plasmid constructed by Feng[19] was used as a wild-type template. All operations were performed according to the manufacturer's protocol (TransGen Biotech). The accuracy of the desired mutations was confirmed by DNA sequencing. Mutant PDHc-E1 was expressed and purified in the same manner as that used for the wild type.

2.8 Fluorescence spectroscopic analysis

Fluorescence spectroscopic measurements were carried out on a FluoreMax-P fluorescence spectrophotometer (Horiba Jobin Yvon, Longjumeau, France) according to a previously described protocol.[20] Fluorescence quenching of wild-type and mutant PDHc-E1 by different concentrations of the title compounds was measured at an emission of 305-500 nm in a 1-cm cuvette. The excitation wavelength was at 290 nm. To correct for background interference, wild-type or mutant PDHc-E1 in buffer was used as a control. The binding constant K_a was calculated using the following formula: $\ln [(F_0 - F) / F] = \ln Ka + n \ln [Q]$, where F_0 and F are the fluorescence intensities of protein in the absence and presence of the title compounds, respectively, and [Q] is the concentration of the quencher. A plot of $\ln [(F_0 - F) / F]$ vs. $\ln [Q]$ gave a straight line using least squares analysis. The intercept on the Y-axis was equal to the log value of K_a.

2.9 Determination of inhibition types

A series of experiments was performed to determine the inhibition kinetics of **4c** and **6d**. The inhibitor concentrations of **4c** were 0, 10, and 20 μM and those of **6d** were 0, 5, and 10 μM. Substrate (ThDP) concentrations were 0, 0.1, 0.2, 0.4, 0.8, 2, 4, 10, 16, 20, 30, 50, and 100 μM in all kinetic studies. Pre-incubation and measurement times were the same as described in section 2.7. DMSO was used as a blank control for background correction. The reaction velocity was calculated using the following formula: $V = \Delta OD_{600} / (K \times 5)$, where ΔOD_{600} is the absorbance difference at 600 nm over 5 min, K is the slope of the DCPIP standard curve, and 5 is the reaction time of the kinetic experiments. A similar set of experiments in the absence of inhibitors **4c** and **6d** was also performed under the same conditions. The kinetic parameters V_{max} and K_m were obtained by curve fitting according to the classical Michaelis-Menten equation.

2.10 Molecular docking

The crystal structure of the PDHc-E1 (PDB code: 1L8A) was obtained from the PDB data base (Protein Data Bank, https://www.rcsb.org/). Hydrogen atoms were first added to the protein using the PDB2PQR server.[21] ThDP and hit compounds were constructed and optimized with Gasteiger charges using SYBYL7.0 and then docked into the active pocket of the prepared PDHc-E1 using Surflex-Dock.[14] AutoDock 4.2[22] was used to investigate the binding modes of the newly developed compounds.

2.11 *In vivo* anti-algal assay

Synechocystis sp. PCC6803, *Microcystis* sp. FACHB905, *Anabaena* sp. FACHB82, *Aphanizomenon* sp. FACHB1395, and *Nostoc* sp. FACHB713 were cultured in 96-well microplates according to a previously described method.[2] The inhibition rate of the title compounds against the five cyanobacteria species was estimated using the following formula:

inhibition (%) = {1− [$\Delta OD_{t,680}$− $\Delta OD_{i,680}$] / $\Delta OD_{o,680}$}×100, where, $\Delta OD_{o,680}$ and $\Delta OD_{t,680}$ are absorbance differences at 680 nm of the cyanobacteria in the blank control and title compounds amended cultures, respectively, and $\Delta OD_{i,680}$ is the absorbance difference at 680 nm of the best compound in each assay. Half maximal effective concentrations (EC_{50}) were estimated with logistic fitting. DMSO was used as a blank control. The commonly used algicides prometryn and copper sulfate, and compound **IV-21l** (R^1 = I, R = 6-Br) (**Fig.1**), which displayed the best inhibition against PCC6803 (EC_{50} = 0.7 μM) in our previous study,[14] served as positive controls.

3 Results and Discussion

3.1 Chemistry

3.1.1 Synthesis

Sixteen novel ThDP analogs in the series of **4** and **6** were designed and synthesized (**Scheme 1**). The synthetic routes are rather simple and convenient.

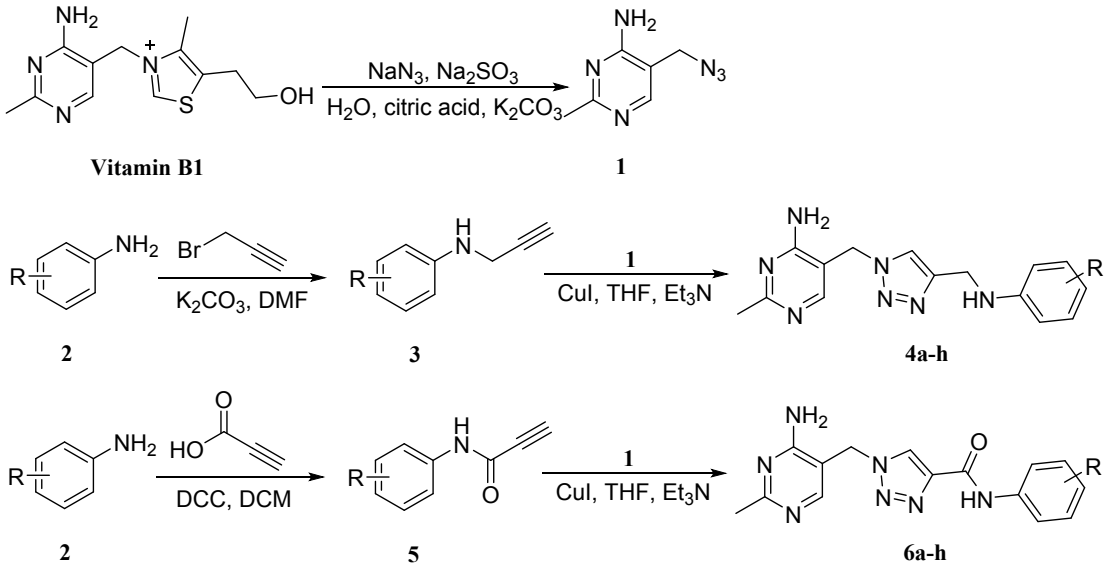

Scheme 1. Synthesis of the title compounds **4** and **6**

In this synthetic route, compound **1**, which was synthesized from thiamine hydrochloride, was in turn an important intermediate in the synthesis of **4** and **6**. The skeleton of title compounds

4 and **6** contains a 1,2,3-triazole ring, which can be readily constructed *via* "click chemistry", a concept introduced by Noble laureate K. Barry Sharpless.[23, 24] In the work presented here, series **4** and **6** were synthesized from **1** *via* a 1,3-dipolar cycloaddition reaction that employed copper(I) iodide and triethylamine in conjunction with terminal alkynes **3** and **5**, respectively. Copper(I) iodide acts as a catalyst in this process, in which Cu^+ catalyzes the reaction of terminal alkynes and azide groups to form 1,2,3-triazole ring.[25, 26] Compounds **3** were prepared by the reaction of propargyl bromide with the appropriate substituted anilines in DMF with K_2CO_3 as a base, while compounds **5** were obtained by the condensation of substituted anilines with propiolic acid in the presence of DCC.

Sixteen novel title compounds were smoothly synthesized by the above-mentioned synthetic method, which had the advantages of being simple, mild, easy and efficient. The generated compounds were fully characterized by ^{1}H NMR, ^{19}F NMR, and HRMS and confirmed by elemental analysis.

3.1.2 Crystal structure of compound 4b

Crystal data for **4b** are presented in **Table 1**, while **Fig. 3** provides a perspective view based on the atomic labeling system (CCDC-1536365; these data are available free of charge from the Cambridge Crystallographic Data Centre). According to the structural analysis, **4b** has a U shaped conformation, which is close to its binding pose.

3.2 Enzyme inhibitory activity against *E. coli* PDHc-E1

The inhibitory activity of title compounds **4a-h** against *E. coli* PDHc-E1 was evaluated. The resulting IC_{50} values, which are summarized in **Table 2**, suggested that the inhibition of **4a-h** could be improved by introducing an imine group into the linker portion. The structural skeleton

of **4** was accordingly further optimized by introducing an amide group as a linker to generate the series **6a-h**.

We found that the inhibitory activity was further enhanced by changing the imine group into an amide group. All compounds in series **6** had higher inhibitory activities than those of series **4** and lead compound **I**. For a given R group, compounds with an amide linkage, i.e., **6a** (R = H, IC_{50} = 14.70 ± 0.14 μM), **6b** (R = 3-Cl, IC_{50} = 9.48 ± 0.25 μM), **6c** (R = 4-Cl, IC_{50} = 7.12 ± 0.08 μM), **6d** (R = 3-Br, IC_{50} = 4.13 ± 0.26 μM), **6g** (R = 3-CF_3, IC_{50} = 7.41 ± 0.01 μM), and **6h** (R = 4-CH_3, IC_{50} = 10.06 ± 0.17 μM), had higher inhibitory activities than the corresponding compounds with an imine group, i.e., **4a** (R = H, IC_{50} = 46.32 ± 0.24 μM), **4c** (R = 3-Cl, IC_{50} = 11.53 ± 0.33 μM), **4d** (R = 4-Cl, IC_{50} = 15.54 ± 0.01 μM), **4e** (R = 3-Br, IC_{50} = 10.91 ± 0.65 μM), **4f** (R = 3-CF_3, IC_{50} = 15.74 ± 0.14 μM), and **4h** (R = 4-CH_3, IC_{50} = 23.76 ± 0.01 μM). We observed that compounds in both series **4** and **6** with an electron-withdrawing R group, i.e., Br, F, Cl, or CF_3, displayed higher inhibition than their counterparts containing the electron-donating R group CH_3. Compounds with no substitution on the benzene ring, such as **4a** and **6a,** showed the weakest inhibition in both series **4** and **6**. The highest inhibitory activity, an IC_{50} value of 4.13 μM, was exhibited by **6d**, which had 3-Br as the R group. According to our results, the linker between the 1,2,3-triazole and benzene ring in the parent structure played a critical role in the inhibition against *E. coli* PDHc-E1. Compared with an ether group, the use of an imine group or amide group as a linker was much more beneficial to the inhibitory activity.

3.3 Inhibitory mechanisms of 4 and 6

To determine the inhibitory mechanisms of series **4** and **6**, compounds **4c** and **6d** were chosen and their kinetic inhibitions on *E. coli* PDHc-E1 were studied. We determined the maximum

velocity (V_{max}) and Michaelis constant (K_m) in the presence and absence of either **4c** or **6d**.

Michaelis-Menten equation curves are shown in **Fig. 4**, and V_{max} and K_m are listed in **Table 3**. As indicated by **Table 3**, V_{max} remained nearly constant whether **4c** or **6d** was in the presence or absence, while K_m increased as the concentration of either **4c** or **6d** was increased. On the basis of these observations, we conclude that **4c** and **6d** act as competitive inhibitors of ThDP against *E. coli* PDHc-E1.

3.4 Selectivity

Many ThDP analogs with poor enzyme selectivity, such as thiamine thiothiazolone pyrophosphate have been reported to have high inhibitory activity against both *E. coli* PDHc-E1 (K_i = 64 nM) and human PDHc-E1 (K_i = 74 nM).[27] Determining the inhibition selectivity of our candidates between mammals and *E. coli* PDHc-E1 is thus important. We selected porcine PDHc-E1 as a mammalian target because its sequence is 98.5% similar to that of human PDHc-E1. Compounds **4c**, **4e**, **6d**, and **6e**, which had good inhibitory activity against both *E. coli* PDHc-E1 and cyanobacteria, were chosen for the enzyme-selectivity examination. We found that these compounds exhibited 100% inhibition against *E. coli* PDHc-E1 at 100 μM, but their inhibition was negligible (<19%) against porcine PDHc-E1. The excellent selectivity of these new ThDP analogs indicates they may have low mammalian toxicity (**Table 4**).

3.5 Analyses of interactions

To identify the possible binding mode of the title compounds, compounds **4e** and **6d** were docked into the active pocket of PDHc-E1. As shown in **Fig. 5**, compounds **4e** and **6d** occupy the ThDP-binding pocket in a ‘V’ conformation. On the right side of the ‘V’ conformation, the 4-aminopyrimidine ring of **4e** and **6d** forms hydrogen bonds with residues V192, M194, and

396 E571, which is similar to the interactions between ThDP and the corresponding residues.[12] On the
397 left side of the 'V' conformation, the terminal benzene ring of **4e** and **6d** can form cation-π and
398 hydrophobic interaction with K392 and L264, respectively.

399 It was found that **4e** (IC_{50} = 10.91 ± 0.65 μM) and **6d** (IC_{50} = 4.13 ± 0.26 μM) displayed
400 significantly higher inhibition against *E. coli* PDHc-E1 than did **Ib** (IC_{50} = 26.44 ± 1.68 μM). We
401 next investigated the difference in binding when the ether group (the linker) was modified to an
402 imine or amide group. As shown in **Fig. 5**, the benzene ring of **4e** and **6d** can participate in
403 hydrophobic interactions with L264, which is obviously different from compound **I**. As illustrated
404 in **Fig. 5B**, a new hydrogen bond between H640 and the N atom of 1,2,3-triazole is additionally
405 formed as a result of the introduction of the amide group, which changes of the structure of **6** and
406 contributes to its better inhibition against PDHc-E1 (IC_{50} = 4.13 μM). In contrast, only a weak
407 intermolecular interaction takes place between **4e** and H640 according to molecular docking
408 analysis.

409 To further confirm the predicted interactions of the title compounds with *E. coli* PDHc-E1, **4e**
410 and **6d** were studied by site-directed mutagenesis and enzymatic assays. The IC_{50} values of **4e** and
411 **6d** against mutants V192A (73.03 and 41.75 μM, respectively), M194A (87.45 and 33.13 μM,
412 respectively), L264A (105.41 and 44.73 μM, respectively), and H640A (25.52 and 22.79 μM,
413 respectively) were much higher than the IC_{50} values against the wild-type PDHc-E1 (10.91 and
414 4.13 μM, respectively) (**Fig. 6**). According to the results, the residues, V192, M194, L264 and
415 H640 play an important role in the binding of **4e** or **6d** with *E. coli* PDHc-E1. PDHc-E1 with an
416 E571A or K392A mutation is completely inactive, however, which prevented the detection of
417 enzyme inhibitory activity. The binding affinity of the title compounds to mutants E571A and

K392A was therefore assessed using fluorescence spectroscopy. The association constant (K_a) of **4e** to mutants E571A and K392A was found to be decreased more than 30 fold, compared with that of **4e** to the wild-type PDHc-E1 (**Table 5**). The binding affinity of **6d** to both mutants was also decreased more than 24 fold (**Table 5**). The above observations indicate that the predictions based on molecular docking were in accord with the experimental results of site-directed mutagenesis.

3.6 Inhibition against cyanobacteria

To examine the practicality of title compounds **4** and **6**, several compounds with acceptable inhibition against *E. coli* PDHc-E1 were selected and evaluated for their anti-cyanobacteria activity. Five algal species (*Synechocystis* sp. PCC6803, *Microcystis* sp. FACHB905, *Anabaena* sp. FACHB82, *Aphanizomenon* sp. FACHB1395, and *Nostoc* sp. FACHB713) with agricultural and environmental significance were used for this assay. Prometryn (a commercial herbicide) and copper sulfate, two algicides currently in common use, were used as positive controls. Compound **IV-21l** (R^1= I, R = 6-Br) (**Fig.1**), which displayed the best inhibition against PCC6803 (EC_{50} = 0.7 μM) in our previously published study,[14] was also selected as a positive control.

As shown in **Table 6**, most compounds in series **4** and **6** had poor inhibition against FACHB713, but all title compounds except **4a** showed a broad spectrum of algicidal activity against four of the algal species (PCC6803, FACHB905, FACHB82, and FACHB1395). Compounds **4b-4h** and **6a-6d** had better potency against PCC6803 and FACHB905 than did prometryn. For example, **4c**, **4e**, **4g**, **4h**, **6d**, **6e**, and **6g**, with EC_{50} < 3 μM, showed stronger inhibition against both algal species than did prometryn (PCC6803, EC_{50} = 13.1±0.7; FACHB905, 14.7 ± 0.8 μM). The algicidal activity of **4c** (EC_{50} = 1.7 ± 0.2 μM) against PCC6803 was also

comparable to that of copper sulfate (EC_{50} = 1.8 ± 0.1 μM). Moreover, **6d** not only exhibited much higher algicidal activity (PCC6803, EC_{50} = 1.6 ± 0.3 μM; FACHB905, EC_{50} = 2.2 ± 0.2 μM; FACHB82, EC_{50} = 1.2 ± 0.1 μM; FACHB1395, EC_{50} = 1.3 ± 0.3 μM) than prometryn but also had activity comparable to or higher than that of copper sulfate (PCC6803, EC_{50} = 1.8 ± 0.1 μM; FACHB905, 1.5 ± 0.1 μM; FACHB82, EC_{50} = 2.8 ± 0.3 μM; FACHB1395, EC_{50} = 1.6 ± 0.1 μM). Although the previously reported compound **IV-21l** showed excellent inhibition against PCC6803 (EC_{50} = 0.7 ± 0.1 μM) and FACHB713 (EC_{50} = 7.8 ± 2.2 μM), its inhibitory activity against FACHB905 (EC_{50} = 4.4 ± 0.2 μM), FACHB82 (EC_{50} = 9.2 ± 1.1 μM) and FACHB1395 (EC_{50} = 4.5 ± 0.2 μM) was significantly lower than that of compound **6d**. It's worth noting that compound **IV-21l** should be synthesized by a six-step sequence starting from 2-amino-5-bromobenzoic acid. However, it takes only three steps to synthesize compound **6d.** The synthesis of **6d** has the advantage of being simple and easy. In addition, **IV-21l** has poor water- and fat-solubility because of its three different nitro-containing heterocycles. Overall, **6d** is a better candidate for further study than **IV-21l**.

The inhibitory potency of the title compounds against cyanobacteria seems to be positively well correlated with their inhibition against *E. coli* PDHc-E1. Compounds with higher levels of *E. coli* PDHc-E1 inhibition displayed stronger potency against the different cyanobacterial species. For instance, **4b-h** and **6a-h** exhibited higher levels of inhibition against *E. coli* PDHc-E1 (IC_{50} = 4.13-23.76 μM) and also exhibited good potency against PCC6803 (EC_{50} = 1.6-4.4 μM) and FACHB905 (EC_{50} = 2.1-8.5 μM). In particular, **6d**, which had the best inhibition against *E. coli* PDHc-E1, also displayed potent inhibition against PCC6803, FACHB905, FACHB82, and FACHB1395. The reverse was true for compounds **I** and **4a**, which had lower levels of enzyme

462 inhibition (IC_{50} > 26 μM) and lower algicidal activities (EC_{50} > 50 μM). These results indicate that
463 an effective algicide can be developed by designing a potent *E. coli* PDHc-E1 inhibitor.

464 **Acknowledgments**

465 The work was supported in part by the National Research and Development Plan
466 (2017YFD0200506), the National Natural Science Foundation of China (21877047, 31701820,
467 21472062, and 21907035), the 111 Project B17019, the Natural Science Foundation of Hubei
468 Province of China (2017CFB232), the National Key Research Development Program of China
469 (2018YFD0200100).

REFERENCES

(1) Yu, Y.; Zeng, Y. D.; Li, J.; Yang, C. Y.; Zhang, X. H.; Luo, F.; Dai, X. Z. An algicidal *Streptomyces amritsarensis* strain against *Microcystis aeruginosa* strongly inhibits microcystin synthesis simultaneously. *Sci. Total Environ*. **2019**, *650*, 34-43.

(2) Li, D.; Han, X. Y.; Tu, Q. D.; Feng, L. L.; Wu, D.; Sun, Y.; Chen, H. F.; Li, Y. J.; Ren, Y. L.; Wan, J. Structure-Based Design and Synthesis of Novel Dual-Target Inhibitors against Cyanobacteria Fructose-1,6-Bisphosphate Aldolase and Fructose-1,6-Bisphosphatase. *J. Agric. Food Chem*. **2013**, *61*, 7453-7461.

(3) Li, H.; Pan, G. Simultaneous Removal of Harmful Algal Blooms and Microcystins Using Microorganism- and Chitosan-Modified Local Soil. *Environ. Sci. Technol*. **2015**, *49*, 6249-6256.

(4) Dalu, T.; Wasserman, R. J. Cyanobacteria dynamics in a small tropical reservoir: Understanding spatio-temporal variability and influence of environmental variables. *Sci. Total Environ*. **2018**, *643*, 835-841.

(5) Saraf, S. R.; Frenkel, A.; Harke, M. J.; Jankowiak, J. G.; Gobler, C. J.; McElroy, A. E. Effects of *Microcystis* on development of early life stage Japanese medaka (*Oryzias latipes*): Comparative toxicity of natural blooms, cultured *Microcystis* and microcystin-LR. *Aquat. Toxicol*. **2018**, *194*, 18-26.

(6) Sun, Y.; Zhang, R.; Li, D.; Feng, L. L.; Wu, D.; Feng, L. N.; Huang, P. P.; Ren, Y. L.; Feng, J. T.; Xiao, S.; Wan, J. Pharmacophore-Based Virtual Screening and Experimental Validation of Novel Inhibitors against Cyanobacterial Fructose-1,6-/Sedoheptulose-1,7-bisphosphatase. *J. Chem. Inf. Model*. **2014**, *54*, 894-901.

(7) Han, X. Y.; Zhu, X. Y.; Zhu, S. H.; Wei, L.; Hong, Z. Q.; Guo, L.; Chen, H. F.; Chi, B.; Liu,

Y.; Feng, L. L.; Ren, Y. L.; Wan, J. A Rational Design, Synthesis, Biological Evaluation and Structure-Activity Relationship Study of Novel Inhibitors against Cyanobacterial Fructose-1,6-bisphosphate Aldolase. *J. Chem. Inf. Model*. **2016**, *56*, 73-81.

(8) Matthijs, H. C. P.; Jančula, D.; Visser, P. M.; Maršálek, B. Existing and emerging cyanocidal compounds: new perspectives for cyanobacterial bloom mitigation. *Aquat. Ecol*. **2016**, *50*, 443-460.

(9) Nemeria, N.; Baykal, A.; Joseph, E.; Zhang, S.; Yan, Y.; Furey, W.; Jordan, F. Tetrahedral Intermediates in Thiamin Diphosphate-Dependent Decarboxylations Exist as a 1',4'-Imino Tautomeric Form of the Coenzyme, Unlike the Michaelis Complex or the Free Coenzyme. *Biochemistry* **2004**, *43*, 6565-6575.

(10) Patel, M. S.; Korotchkina, L. G. The Biochemistry of the Pyruvate Dehydrogenase Complex. *Biochem. Mol. Biol. Educ*. **2003**, *31*, 5-15.

(11) Balakrishnan, A.; Nemeria, N. S.; Chakraborty, S.; Kakalis, L.; Jordan, F. Determination of Pre-Steady-State Rate Constants on the *Escherichia coli* Pyruvate Dehydrogenase Complex Reveals That Loop Movement Controls the Rate-Limiting Step. *J. Am. Chem. Soc*. **2012**, *134*, 18644-18655.

(12) Arjunan, P.; Nemeria, N.; Brunskill, A.; Chandrasekhar, K.; Sax, M.; Yan, Y.; Jordan, F.; Guest, J. R.; Furey, W. Structure of the Pyruvate Dehydrogenase Multienzyme Complex E1 Component from *Escherichia coli* at 1.85Å Resolution. *Biochemistry* **2002**, *41*, 5213-5221.

(13) He, J. B.; Feng, L. L.; Li, J.; Tao, R. J.; Wang, F.; Liao, X.; Sun, Q. S.; Long, Q. W.; Ren, Y. L.; Wan, J.; He, H. W. Design, synthesis and biological evaluation of novel 2-methylpyrimidine-4-ylamine derivatives as inhibitors of *Escherichia coli* pyruvate

dehydrogenase complex E1. *Bioorg. Med. Chem*. **2012**, *20*, 1665-1670.

(14) Zhou, Y.; Feng, J. T.; He, H. W.; Hou, L. F.; Jiang, W.; Xie, D.; Feng, L. L.; Cai, M.; Peng, H. Design, Synthesis, and Potency of Pyruvate Dehydrogenase Complex E1 Inhibitors against Cyanobacteria. *Biochemistry* **2017**, *56*, 6491-6502.

(15) Erixon, K. M.; Dabalos, C. L.; Leeper, F. J. Synthesis and biological evaluation of pyrophosphate mimics of thiamine pyrophosphate based on a triazole scaffold. *Org. Biomol. Chem*. **2008**, *6*, 3561-3572.

(16) Majumdar, K. C.; Ganai, S. An expedient approach to substituted triazole[1,5-*α*][1,4] benzodiazepines via Cu-catalyzed tandem Ullmann C-N coupling/azide-alkyne cycloaddition. *Tetrahedron Lett*. **2013**, *54*, 6192-6195.

(17) Ramachandran, P. V.; Rudd, M. T.; Reddy, M. V. R. Stereoselective synthesis of hex-2-(*E*)-en-4-yn-1,6-dioates and *E,Z*-muconic acid diesters via organo-catalyzed self-coupling of propiolates. *Tetrahedron Lett*. **2005**, *46*, 2547-2549.

(18) Ren, Y. L.; He, J. B.; Feng, L. L.; Liao, X.; Jin, J.; Li, Y. J.; Cao, Y.; Wan, J.; He, H. W. Structure-based rational design of novel hit compounds for pyruvate dehydrogenase multienzyme complex E1 components from *Escherichia coli*. *Bioorg. Med. Chem*. **2011**, *19*, 7501-7506.

(19) Feng, L. L.; Sun, Y.; Deng, H.; Li, D.; Wan, J.; Wang, X. F.; Wang, W. W.; Liao, X.; Ren, Y. L.; Hu, X. P. Structural and biochemical characterization of fructose-1,6/sedoheptulose-1,7-bisphosphatase from the cyanobacterium *Synechocystis* strain 6803. *FEBS J*. **2014**, *281*, 916-926.

(20) Feng, L. L.; He, J. B.; He, H. F.; Zhao, L. L.; Deng, L. F.; Zhang, L.; Zhang, L.; Ren, Y. L.; Wan, J.; He, H. W. The design, synthesis and biological evaluation of novel thiamin diphosphate

analog inhibitors against the pyruvate dehydrogenase multienzyme complex E1 from *Escherichia coli*. *Org. Biomol. Chem*. **2014**, *12*, 8911-8918.

(21) Dolinsky, T. J.; Nielsen, J. E.; McCammon, J. A.; Baker, N. A. PDB2PQR: an automated pipeline for the setup of Poisson-Boltzmann electrostatics calculations. *Nucleic Acids Res*. **2004**, *32*, 665-667.

(22) Morris, G. M.; Huey, R.; Lindstrom, W.; Sanner, M. F.; Belew, R. K.; Goodsell, D. S.; Olson, A. J. AutoDock4 and AutoDockTools4: Automated Docking with Selective Receptor Flexibility. *J. Comput. Chem*. **2009**, *30*, 2785-2791.

(23) Kolb, H. C.; Finn, M. G.; Sharpless, K. B. Click Chemistry: Diverse Chemical Function from a Few Good Reactions. *Angew. Chem. Int. Ed*. **2001**, *40*, 2004-2021.

(24) Wu, P.; Malkoch, M.; Hunt, J. N.; Vestberg, R.; Kaltgrad, E.; Finn, M. G.; Fokin, V. V.; Sharpless, K. B.; Hawker, C. J. Multivalent, bifunctional dendrimers prepared by click chemistry. *Chem. Commun*. **2005**, *37*, 5775-5777.

(25) Rostovtsev, V. V.; Green, L. G.; Fokin, V. V.; Sharpless, K. B. A Stepwise Huisgen Cycloaddition Process: Copper(I)-Catalyzed Regioselective "Ligation" of Azides and Terminal Alkynes. *Angew. Chem. Int. Ed*. **2002**, *41*, 2596-2599.

(26) Himo, F.; Lovell, T.; Hilgraf, R.; Rostovtsev, V. V.; Noodleman, L.; Sharpless, K. B.; Fokin, V. V. Copper(I)-Catalyzed Synthesis of Azoles. DFT Study Predicts Unprecedented Reactivity and Intermediates. *J. Am. Chem. Soc*. **2005**, *127*, 210-216.

(27) Nemeria, N.; Yan, Y.; Zhang, Z.; Brown, A. M.; Arjunan, P.; Furey, W.; Guest, J. R.; Jordan, F. Inhibition of the *Escherichia coli* Pyruvate Dehydrogenase Complex E1 Subunit and Its Tyrosine 177 Variants by Thiamin 2-Thiazolone and Thiamin 2-Thiothiazolone Diphosphates. *J.*

Biol. Chem. **2001**, *276*, 45969-45978.

Tables

Table 1. Crystallographic data of compound **4b**.

Parameters	Data
chemical formula	$C_{15}H_{16}ClN_7$
formula weight	329.80
crystal system	monoclinic
space group	P2(1)/c
crystal color	colorless
a (Å)	14.488(4)
b (Å)	9.884(2)
c (Å)	12.319(3)
α (deg)	90
β (deg)	115.098(4)
γ (deg)	90
V (Å)	1597.6(7)
Z	4
D_{calc} ($Mg \cdot m^{-3}$)	1.371
θ range (deg)	2.58-26.00
hkl range	$-17 \le h \le 16$; $-12 \le k \le 12$; $-15 \le l \le 15$
F (0 0 0)	688
no. collected refl.	14090
no. ind. Refl. (R_{int})	3126 (0.0908)
data/ restraints/ parameters	3126 / 0 / 209
Absorption coefficient (mm^{-1})	0.250
R1; wR_2 [$I > 2\sigma(I)$]	0.0500; 0.1225
R1; wR_2 (all data)	0.0776; 0.1434
GOOF	1.015

Table 2. Structure and inhibitory activity of **I**, **4**, and **6**

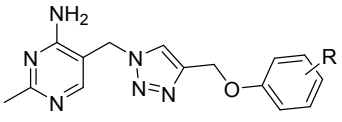

L

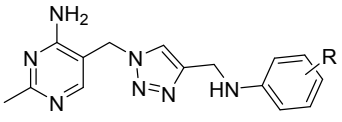

4

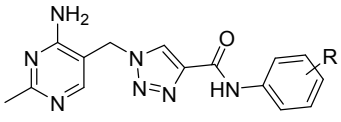

6

Compd.	R	IC_{50} (μM) Inhibitory against *E. coli* PDHc-E1	Compd.	R	IC_{50} (μM) Inhibitory against *E. coli* PDHc-E1
L1	H	55.15 ± 4.65	**4h**	4-CH_3	23.76 ± 0.01
L2	4-Cl	26.44 ± 1.68	**6a**	H	14.70±0.14
L3	3-CF_3	32.73 ± 0.17	**6b**	3-Cl	9.48 ± 0.25
4a	H	46.32 ± 0.24	**6c**	4-Cl	7.12 ± 0.08
4b	2-Cl	13.41 ± 0.82	**6d**	3-Br	4.13 ± 0.26
4c	3-Cl	11.53 ± 0.33	**6e**	4-Br	5.65 ± 0.01
4d	4-Cl	15.54 ± 0.01	**6f**	4-F	5.92 ± 0.02

4e	3-Br	10.91 ± 0.65	**6g**	3-CF_3	7.41 ± 0.01
4f	3-CF_3	15.74 ± 0.14	**6h**	4-CH_3	10.06 ± 0.17
4g	4-CF_3	14.08 ± 0.89			

Table 3. V_{max} and K_m values of compounds **4c** and **6d** against *E. coli* PDHc-E1

Compd.	Concentration (μM)	V_{max} (μM/min/mg)	K_m (μM)
4c	0	7.05 ± 0.17	2.49 ± 0.27
	10	7.53 ± 0.54	6.91 ± 1.32
	20	7.10 ± 0.43	29.44 ± 2.24
6d	0	8.24 ± 0.72	2.9 ± 1.14
	5	7.62 ± 0.23	5.27 ± 0.52
	10	7.69 ± 0.29	19.13 ± 1.06

Table 4. Inhibition of **4** and **6** against *E. coli* and porcine PDHc-E1

Compd.	*E. coli* PDHc-E1		Porcine PDHc-E1
	IC_{50}(μM)	Inhibitory potency † (%)	Inhibitory potency † (%)
4c	11.53±0.33	100.00±0.05	9.48±0.25
4e	10.91±0.65	100.00±0.36	11.76±0.14
6d	4.13±0.26	100.00±0.06	16.41±0.01
6e	5.65±0.01	100.00±0.01	18.06±0.17

†, Inhibitory potency (%) of compounds against enzyme *in vitro* at 100 μM as average of triplicate.

Table 5 The association constant (*Ka*) for **4e** and **6d** binding to PDHc-E1 with K392A and E571A mutation

Mutation type	$Ka \times 10^5$ M^{-1}	
	4e	**6d**
WT	72.7	14.7
K392A	1.7	0.59
E571A	2.3	0.43

Table 6. Structures and EC_{50} values against cyanobacteria of compounds **I**, **4**, **6**, and **IV-21l**

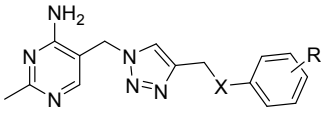

L: X=O; 4: X=NH

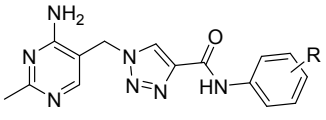

6

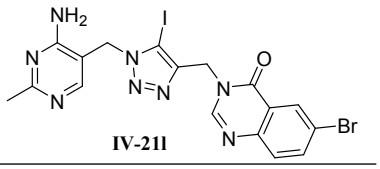

IV-21l

Compd.	**R**	**EC50 (μM)**				
		PCC6803	**FACHB905**	**FACHB82**	**FACHB1395**	**FACHB713**
L1	H	>50	>50	>50	>50	>50
L2	4-Cl	>50	>50	>50	>50	>50
L3	3-CF_3	>50	>50	>50	>50	>50
4a	H	>50	>50	>50	>50	>50
4b	2-Cl	4.2±1.0	8.5±0.4	8.6±2.1	5.5±0.4	>50

4c	3-Cl	1.7±0.2	4.9±0.4	10.6±1.7	3.3±0.2	>50
4d	4-Cl	3.3±0.3	3.8±0.1	28.1±15.4	7.5±0.2	>50
4e	3-Br	2.6±0.2	2.1±0.2	>50	>50	>50
4f	3-CF_3	3.8±0.8	4.1±0.3	8.4±1.5	6.5±1.9	8.7±1.2
4g	4-CF_3	2.2±0.1	2.5±0.3	>50	8.0±1.0	>50
4h	4-CH_3	2.2±0.3	2.9±0.8	16.3±2.2	11.1±0.1	>50
6a	H	3.0±0.1	3.2±1.6	>50	5.7±0.3	>50
6b	3-Cl	3.7±0.5	4.3±1.0	>50	6.7±1.4	>50
6c	4-Cl	4.4±0.6	3.9±0.4	>50	15.2±7.7	>50
6d	3-Br	1.6±0.3	2.2±0.3	1.2±0.1	1.3±0.3	>50
6e	4-Br	2.9±0.3	2.8±0.4	>50	12.2±2.3	>50
6f	4-F	3.0±0.8	3.4±0.8	>50	12.5±3.8	>50
6g	3-CF_3	2.7±0.9	2.8±2.4	>50	>50	>50
6h	4-CH_3	2.8±0.4	3.4±0.4	9.0±1.5	5.4±0.3	8.6±0.9
IV-21l		0.7±0.1	4.4±0.2	9.2±1.1	4.5±0.2	7.8±2.2
Prometryne		13.1±0.7	14.7±0.8	19.3±0.4	15.2±0.1	17.9±0.3
$CuSO_4$		1.8±0.1	1.5±0.1	2.8±0.3	1.6±0.1	2.4±0.2

Figures:

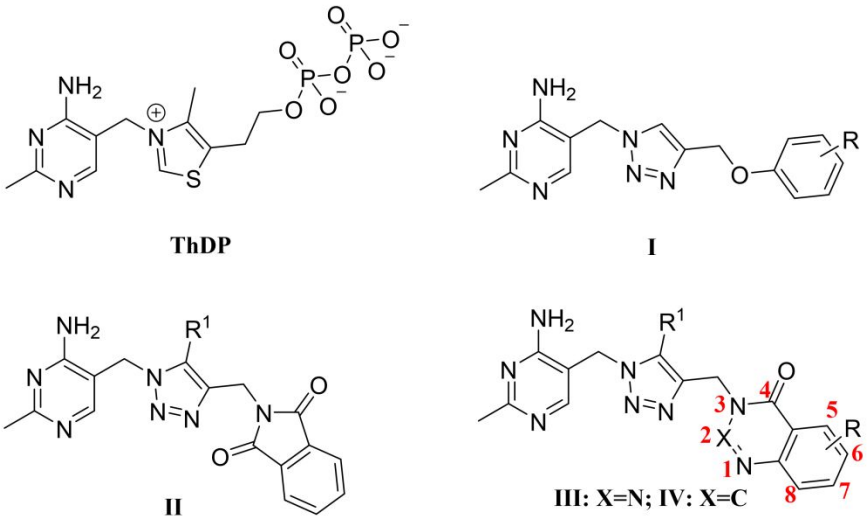

Figure 1. Structures of ThDP and known PDHc-E1 inhibitors.

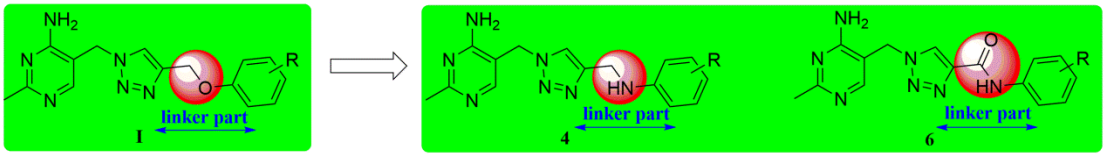

Figure 2. Design of the new 1,2,3-triazole aminopyrimidines **4** and **6**.

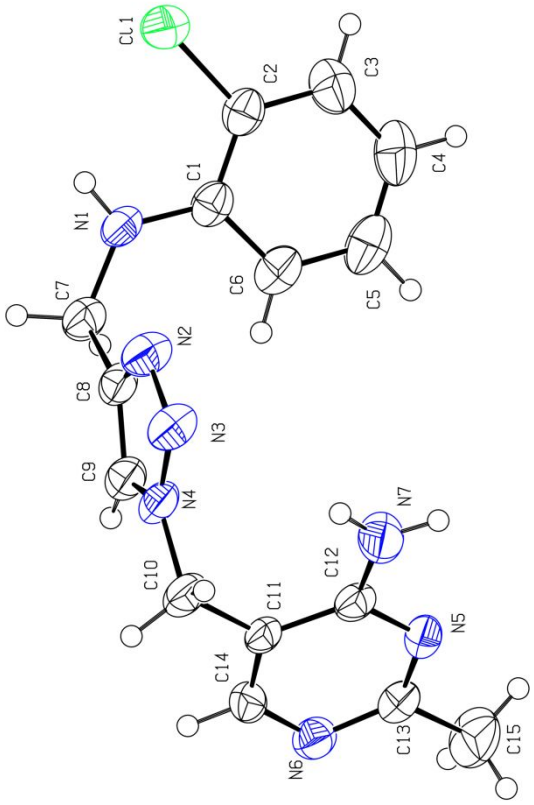

Figure 3. Crystal structure of compound **4b** by X-ray diffraction determination.

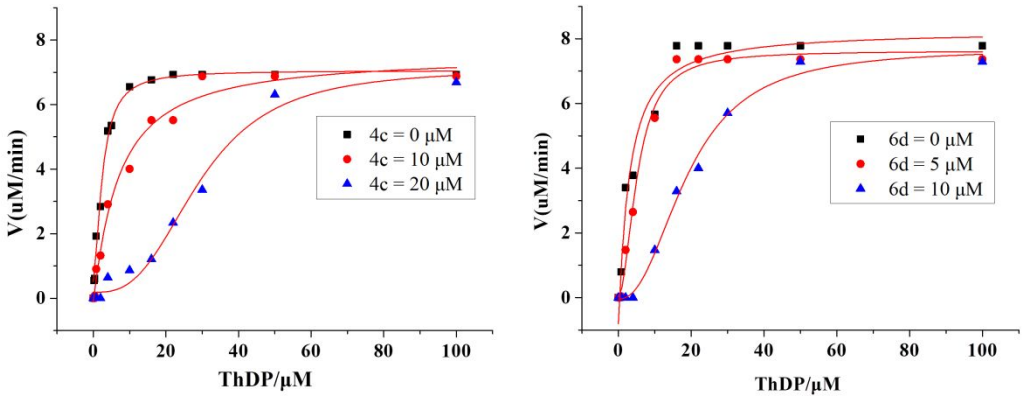

Figure 4. Enzyme kinetic experiments data of **4c** and **6d** against *E. coli* PDHc-E1.

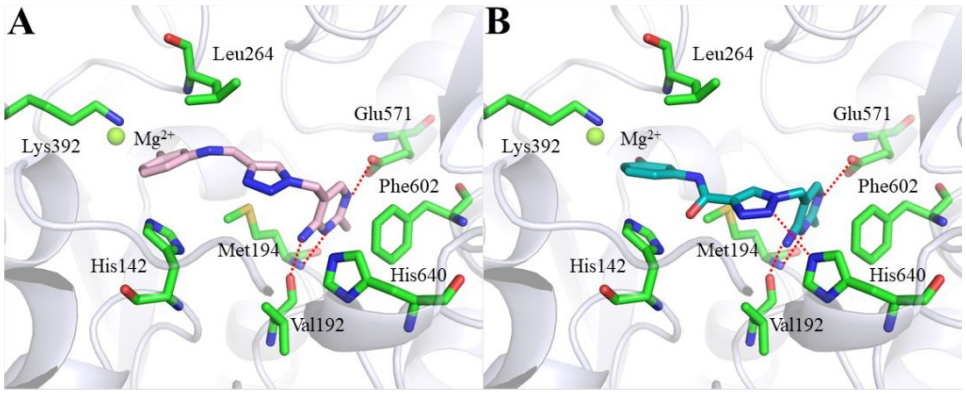

Figure 5. Optimal binding model for compounds **4e** (A) and **6d** (B) at the active site of *E. coli* PDHc-E1 docked by Autodock 4.2. PDHc-E1 is shown as ribbon, ligands and some key residues are shown as stick, and hydrogen bonds are shown as dashed lines.

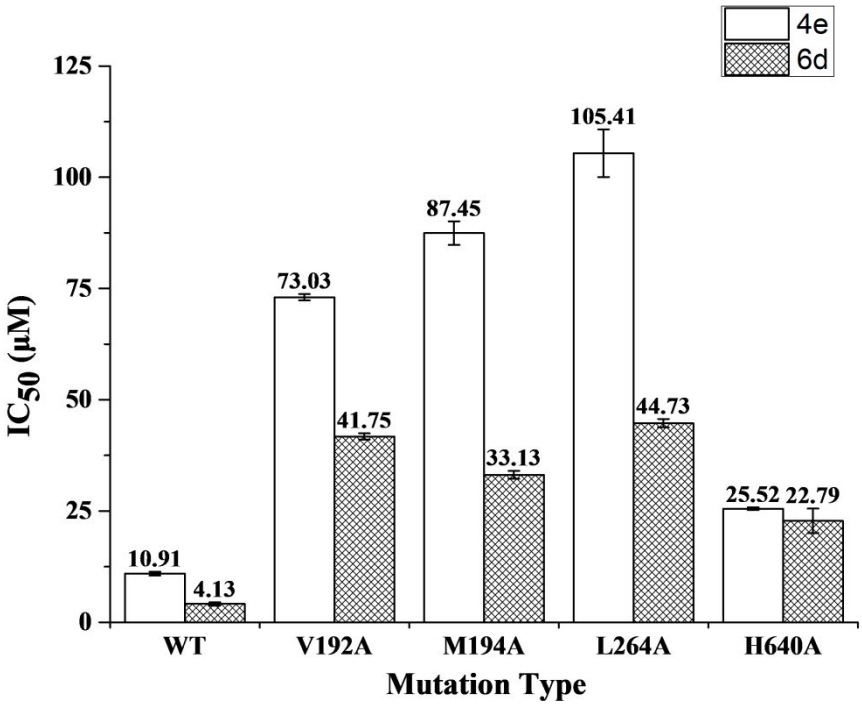

Figure 6. IC_{50} values of **4e** and **6d** against wild type (WT) *E. coli* PDHc-E1 and its mutants. The substrate is pyruvate acid, and the cofactor is ThDP.

Table of Contents Graphic

Synthesis and Activity of 1,2,3-Triazole Aminopyrimidines against Cyanobacteria as PDHc-E1 Competitive Inhibitors

Yuan Zhou[1], Jiangtao Feng[1], Lingling Feng, Dan Xie, Hao Peng, Meng Cai[*], Hongwu He[*]